Draft version February 2, 2008
Preprint typeset using LaTeX style emulateapj v. 6/22/04

arXiv:astro-ph/0409504v1 21 Sep 2004

CORONAL HEATING THROUGH BRAIDING OF MAGNETIC FIELD LINES

Hardi Peter[1]
Kiepenheuer-Institut für Sonnenphysik, 79104 Freiburg, Germany; peter@kis.uni-freiburg.de

Boris V. Gudiksen[2]
Institute of Theoretical Astrophysics, University of Oslo, Norway

Åke Nordlund[3]
Astronomical Observatory, NBIfAFG, University of Copenhagen, Denmark

Draft version February 2, 2008

ABSTRACT

Cool stars like our Sun are surrounded by a million degree hot outer atmosphere, the corona. Since more than 60 years the physical nature of the processes heating the corona to temperatures well in excess of those on the stellar surface remain puzzling. Recent progress in observational techniques and numerical modeling now opens a new window to approach this problem. We present the first coronal emission line spectra synthesized from three-dimensional numerical models describing the evolution of the dynamics and energetics as well as of the magnetic field in the corona. In these models the corona is heated through motions on the stellar surface that lead to a braiding of magnetic field lines inducing currents which are finally dissipated. These forward models enable us to synthesize observed properties like (average) emission line Doppler shifts or emission measures in the outer atmosphere, which until now have not been understood theoretically, even though many suggestions have been made in the past. As our model passes these observational tests, we conclude that the flux braiding mechanism is a prime candidate for being the dominant heating process of the magnetically closed corona of the Sun and solar-like stars.

Subject headings: Sun: corona — stars: coronae — Sun: UV radiation — MHD

1. INTRODUCTION

Shortly after it was realized in the 1930ies that the corona is hot (Grotrian 1939; Edlén 1943), first proposals for the heating mechanism were made based on upward propagating sound waves generated on the stellar surface (Schwarzschild 1948) because convective motions contain far more energy than what is needed to heat the corona. Later it became clear that the heating mechanism has to be related to the magnetic field dominating in the corona. The coronal magnetic field is rooted in the photosphere, however, where it is dominated by the kinetic energy of the convection. Thus at the surface magnetic field-lines are pushed around, and the (stochastic) footpoint motions result in a braiding of the magnetic field lines in the corona. This implies that magnetic field gradients are built up, inducing currents which are finally dissipated and thus heat the corona as suggested by Parker (1972, 1994) — see also Sturrock & Uchida (1981); Parker (1983); van Ballegooijen (1986); Heyvaerts & Priest (1992). Thus the magnetic field acts as the agent to channel energy from the cool surface into the hot corona. Several studies have been carried out to investigate the role of footpoint motions for coronal heating. For example Priest & Schrijver (1999) studied the influence of moving magnetic sources of opposite polarity in the photosphere on reconnection in the above corona and Priest et al. (2002) constructed a model view for coronal heating based on flux-tube tectonics related to the ever changing structure of the magnetic carpet (Schrijver et al. 1998). Many other mechanisms have been discussed to heat the corona, e.g. based on waves, but there are too many of them to be reviewed here (see the SOHO 15 proceedings for an up to date overview, Danesy 2004).

Even though the proposal of field line braiding has been widely discussed, it was not until recently that numerical modeling made it possible to test whether this mechanism actually works. Studies had been conducted for the flux braiding on small scales, investigating the amount and character of the energy deposition (Hendrix et al. 1996; Galsgaard & Nordlund 1996). Finally a small active region could be described in a numerical experiment, resulting in a realistic looking corona consisting of a number of loop-like structures (Gudiksen & Nordlund 2002, 2004b,a).

In this work we go one step further and synthesize emission line spectra from such *ab-initio* coronal models (Fig. 1) and compute average properties of these spectra, especially emission measures and Doppler shifts (Figs. 2, 3), which can be considered as a test for the energetics and the dynamics in the model corona, respectively. This allows a robust comparison of the model not only to the Sun but also to other stars.

2. MHD MODEL AND SPECTRAL SYNTHESIS

The solar atmosphere is modeled from the photosphere to the lower corona using a sixth order fully compressible 3D magneto-hydrodynamics (MHD) code on a staggered non-equidistant mesh. The simulated volume is 60×60 Mm^2 horizontally and 37 Mm vertically. It includes the Spitzer (1956) heat conductivity along the magnetic field, and a cooling function representing radiative losses in

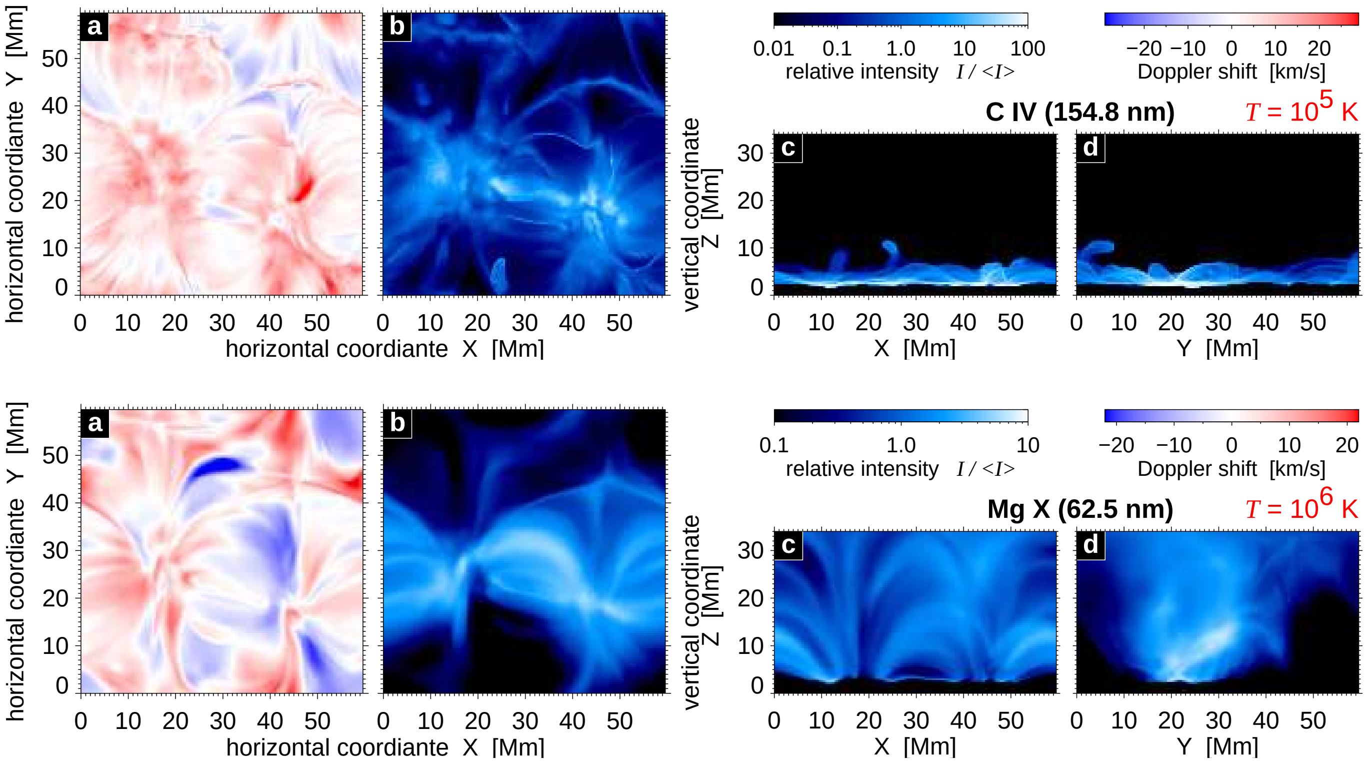

FIG. 1.— Spatial maps in Doppler shift and intensity for the emission lines of C IV at 154.8 nm (top row) and Mg X at 62.5 nm (bottom row). Panels (a) show Doppler shifts of the synthesized spectra as seen from straight above, panels (b) show the same for line intensity. This corresponds to the appearance near the center of the stellar disk. Panels (c) and (d) show side views of the computational box along the x and y axis in line intensity, corresponding to limb observations. The intensities I are scaled according to the average intensity $\langle I\rangle$ of the respective map. Please note the different color tables, especially that the C IV intensity shows much higher contrast than Mg X. Despite the pretty smooth appearance in intensity, the Doppler shift map of Mg X is highly structured.

the optically thin corona. In the optically thick photosphere and chromosphere the temperature is kept near a prescribed temperature profile by a Newtonian temperature relaxation scheme. The initial magnetic field is a potential extrapolation of an MDI/SOHO high resolution magnetogram of AR 9114 scaled to fit into the computational domain. The lower boundary is stressed by a time dependent velocity field, constructed from a Voronoi-tesselation (Okabe et al. 1992), shown to reproduce the granulation pattern (Schrijver et al. 1997). The velocity field reproduces the geometrical pattern as well as the amplitude power spectrum of the velocity and the vorticity leaving no free parameters.

The braiding of the magnetic field by the photospheric motions rapidly produces an intermittent corona in both time and space with a typical temperature of one million K, during the whole simulated timespan of ∼50 minutes. The time and space averaged heating function decreases exponentially with height, producing a heat input to the corona of $2{-}8\times10^3\,\mathrm{W\,m^{-2}}$ in agreement with coronal energy losses estimated from observations (Withbroe & Noyes 1977). The amount of heating produced is constant or if anything rises as numerical resolution increases (Hendrix et al. 1996; Galsgaard & Nordlund 1996) and therefore the amount of heating produced in this simulation is a lower limit. Thus the spatial resolution of the model (400 km) is not sufficient to resolve the reconnection process, of course, but based on the above work the amount of energy input into the corona on larger scales should be of the right order. Details on and results from this MHD model can be found in Gudiksen & Nordlund (2004b,a).

Using density, velocity and temperature from the MHD model the emissivity for a number of emission lines is evaluated at each grid point in the computational domain. By integrating along a line of sight this finally results in maps of spectra when looking at the computational box from, e.g., straight above.

Almost all emission lines from the low corona and transition region are in the extreme ultraviolet (EUV; ≈500-1500Å), optically thin and excited predominantly through electron collisions. The emissivity ε is given through the energy $h\nu$, the Einstein coefficient A_{21} and the upper level population n_2 for the transition from an upper level 2 to a lower level 1, i.e. $\varepsilon = h\nu\, n_2 A_{21}$. To calculate the upper level density one has to evaluate the balances for excitation and ionization. In the latter case we assume ionization equilibrium. We have checked ionization and advection times and found that for the present models ionization equilibrium is a reasonable choice. Furthermore we assume constant abundances with photospheric values. All these quantities, i.e. ionization, excitation, abundances, Einstein coefficients and transition energies, have been evaluated using the atomic data package Chianti (Dere et al. 1997; Young et al. 2003), finally resulting in the emissivity at each grid point depending on the density and temperature there. The spectral profiles at each grid point are assumed to be a Gaussian with a line width correspond-

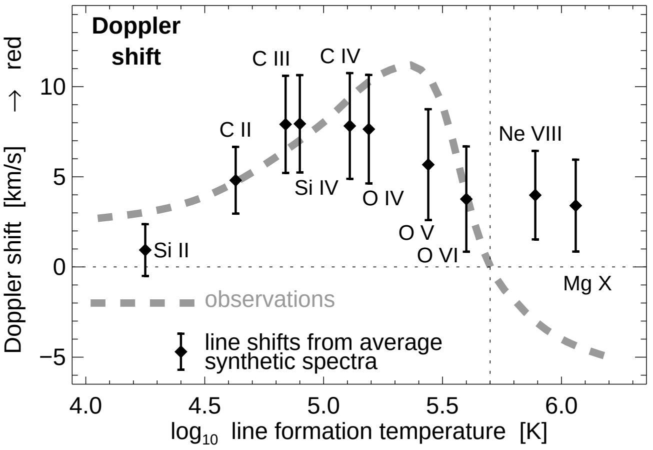

FIG. 2.— Comparison of synthesized and observed Doppler shifts. The diamonds show the Doppler shifts of the temporally and spatially averaged spectra for a number of emission lines formed over temperatures from the transition region and low corona. The bars indicate the standard deviation (scatter) of the Doppler shifts in a time-averaged spatial map when looking from straight above at the computational box (cf. panels a in Fig. 1). The thick dashed line shows the trend as found in observations.

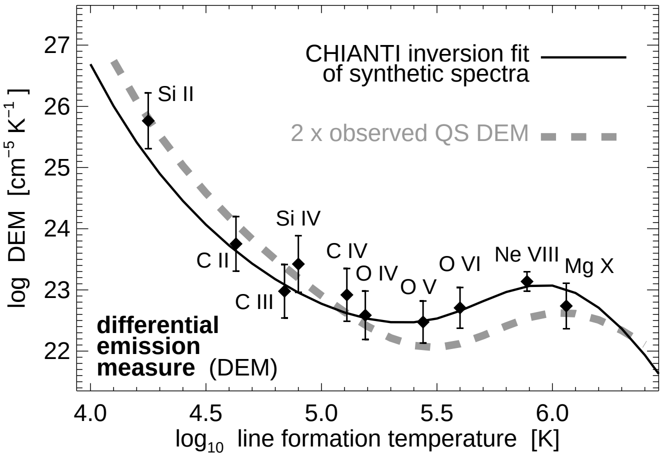

FIG. 3.— Differential emission measure (DEM) as following from the synthesized line intensities compared to observations. The solid line shows the fit from the DEM inversion based on the spatially and temporally averaged synthetic spectra. The bars indicate the standard deviation of line intensities in a spatial map. The thick dashed line is based on a DEM inversion using observed quiet Sun disk center line radiances from SUMER (Wilhelm et al. 1998) scaled by a factor of two to match the active region model.

ing to the thermal width $(2k_{\rm B}T/m)^{1/2}$, where T is the temperature at the respective grid point and m the mass of the ion emitting the line. These Gaussians are shifted by the component of the velocity along the line of sight at the respective grid point. Finally we integrate the spectra along the line of sight (e.g. the vertical direction) to construct a map of spectra.

These synthesized spectral maps can the be analyzed exactly as it is done for observations, e.g. for a spatial scan using the SUMER instrument on-board SOHO (Wilhelm et al. 1995). The resulting spatial maps in line intensity and line shift for a snapshot of the model run can be seen in panels (a) and (b) of Fig. 1 for the lines of C IV at 154.8 nm and Mg X at 62.5 nm, formed around 10^5 K and 10^6 K respectively. The panels (c) and (d) show the intensity images when viewing the box from the sides, i.e. along the x- and y-axis.

3. DISCUSSION

The synthesized corona as shown in Fig. 1 is made up by numerous individual loops, and the appearance is remarkably different in the two lines. At high temperatures the structures are rather washed out and less sharp, partly reflecting that heat conduction ($\propto T^{5/2}$) is very efficient at high temperatures. These findings agree well with real observations, and the synthetic maps roughly resemble maps of solar observations.

Furthermore these images reveal that in the model corona the low temperature emission originates not only from the low parts of the high temperature loops, but that a multitude of low lying cool dense loops are present. Defining the footpoints of the hot loops by circles (covering about 2% of the area) we estimated that only some 10 to 15% of the emission from typical transition region lines formed below 200 000 K originates from that area. Thus the transition region emission is enhanced in the footpoint regions of hot loops, but the majority is emitted in cooler structures. This supports earlier sketches of the structure of the low corona (Dowdy et al. 1986; Peter 2001), but now for the first time this multi-component or multi-loop structure is based on a solid model of the coronal structures.

It is also important to note that the Doppler shift images of the high-temperature line shows much more structures than the intensity image (Fig. 1, panels a and b in lower row), reflecting the highly dynamic nature of the low corona. This shows the importance of using EUV spectrographs with sufficient spectral resolution to learn about the basic coronal processes.

The first major test is provided through average Doppler shifts, which are shown in Fig. 2. The temporally and spatially averaged shifts of synthesized spectra for a number of emission lines are displayed as diamonds. The bars represent the scatter in the spatial maps (standard deviation; cf. Fig. 1). The underlying thick dashed line shows the observed average variation of line shifts with temperature compiled from recent quiet Sun studies (Peter & Judge 1999). Active regions (Teriaca et al. 1999) and a large number of cool stars (Wood et al. 1997; Pagano et al. 2004) show a similar behavior. The coherence of the average Doppler shifts synthesized from the model and the observed ones is remarkable. Also the large scatter is as found with observations (Peter 1999). For the first time the overall variation of Doppler shifts as a function of line formation temperature could be reproduced — the line shifts are caused by flows along the magnetic structures induced by asymetric heating. Many attempts have been made to understand this curve since the first recognition of systematic line shifts in the solar transition region (Doschek et al. 1976). However, many of these models failed (Peter & Judge 1999) and none of them reached the level of qualitative and quantitative agreement achieved by our study.

Only at the highest temperatures does our model not reproduce the recently observationally established blueshifts (Peter 1999; Peter & Judge 1999). This could be due to the influence from the impenetrable upper boundary condition of the MHD model, which may be expected to quench flows along magnetic field lines that intersect the upper boundary. New models, where the upper boundary is shifted higher up into the corona, will further reduce the boundary effects and could provide an even better match to the observed Doppler shifts.

The other major test is to check the emission measure distribution, which describes the emission efficiency at a given temperature and is defined as $n^2\,\mathrm{d}h/\mathrm{d}T$ (for electron density n and temperature gradient with height $\mathrm{d}T/\mathrm{d}h$) (Mariska 1992). Using the synthesized lines (averaged spatially and temporally) we have performed an inversion to obtain the emission measure curve, using the Chianti package (Young et al. 2003). The result is shown as a solid line in Fig. 3. The bars indicate the scatter of the emissivities this inversion is based upon (standard deviation). Over-plotted as a thick dashed line is an inversion from observed quiet Sun spectra of the same lines from SUMER full disk data (Wilhelm et al. 1998). for Mg X we evaluated disk center spectra as no full disk scans exist in this line. The observed quiet Sun emission measure is scaled by a factor of two, to be comparable to our active region calculation.

The agreement of the emission measure curve from the observations and the synthetic spectra is remarkable. Previous (1D or 2D) models failed to reproduce this emission measure curve at low temperatures by orders of magnitude, basically because they had not enough emitting material below 10^5 K. It has been proposed, among other suggestions, that in the lowest corona a large number of cool dense structures might exist (Gabriel 1976; Dowdy et al. 1986). This proposition is supported by our results, where enough energy is released very low in the corona and transition region so that enough dense cool structures form. Thus we can unambiguously reproduce the high emission measures at low temperatures, for the first time without any fine-tuning. As the emission measure curve is a general feature of a large variety of cool stars including our Sun, this suggests that the flux-braiding mechanism may be important in a wide variety of cool stars.

Future work will have to concentrate on improving the coronal MHD model as well as the spectral synthesis. This includes the addition of the super-granular structures to the active region patterns, which is of vital importance to understand the structure of the quiet solar corona. Furthermore larger scale shear motions would be needed to achieve a higher level of activity. In this case the plasma motions are expected to be faster, and therefore requiring the inclusion of non-equilibrium ionization effects when calculating the emission line spectra.

4. CONCLUSIONS

This work is the first to reproduce the Doppler shifts and emission measure distributions in the corona of the Sun and many cool stars in a quantitative and qualitative way. Further work will be needed to apply the model also to a wider variety of stellar activity, especially when thinking of stars with different magnetic field structures (Donati et al. 1999) or convection patterns (Freytag et al. 2002) on the stellar surface. This will show in which types of cool star coronae this heating mechanism is the dominant one. But already we can conclude that flux braiding is a prime candidate for heating in the magnetically closed parts of the coronae of the Sun and solar-like stars.

Computing time for the MHD-modeling was provided by the Swedish National Allocations Committee and by the Danish Center for Scientific Computing.

REFERENCES

Danesy, D., ed. 2004, Coronal Heating — Proceedings of the SOHO 15 conference, ESA SP-575 (ESA Publications Division)
Dere, K. P., Landi, E., Mason, H. E., Monsignori Fossi, B. C., & Young, P. R. 1997, A&AS, 125, 149
Donati, J.-F., Collier Cameron, A., Hussain, G. A. J., & Semel, M. 1999, MNRAS, 302, 437
Doschek, G. A., Feldman, U., & Bohlin, J. D. 1976, ApJ, 205, L177
Dowdy, J. F., Rabin, D., & Moore, R. L. 1986, Sol. Phys., 105, 35
Edlén, B. 1943, Zeitschrift f. Astrophys., 22, 30
Freytag, B., Steffen, M., & Dorch, B. 2002, Astronomische Nachrichten, 323, 213
Gabriel, A. H. 1976, Phil. Trans. Roy. Soc. Lond., A 281, 339
Galsgaard, K. & Nordlund, Å. 1996, J. Geophys. Res., 101, 13445
Grotrian, W. 1939, Naturwiss., 27, 214
Gudiksen, B. & Nordlund, Å. 2002, ApJ, 572, L113
—. 2004a, ApJ, submitted, astro-ph/0407266
—. 2004b, ApJ, submitted, astro-ph/0407267
Hendrix, D. L., van Hoven, G., Mikic, Z., & Schnack, D. D. 1996, ApJ, 470, 1192
Heyvaerts, J. & Priest, E. R. 1992, ApJ, 390, 297
Mariska, J. T. 1992, The solar tansition region (Cambridge Univ. Press, Cambridge)
Okabe, A., Boots, B., & Sugihara, K. 1992, Spatial tessellations. Concepts and applications of voronoi diagrams (Wiley Series in Probability and Mathematical Statistics, Chichester, New York)
Pagano, I., Linsky, J. L., Valenti, J., & Duncan, D. K. 2004, A&A, 415, 331
Parker, E. N. 1972, ApJ, 174, 499
—. 1983, ApJ, 264, 642
—. 1994, Spontaneous current sheets in magnetic fields (Oxford University Press)
Peter, H. 1999, ApJ, 516, 490
—. 2001, A&A, 374, 1108
Peter, H. & Judge, P. G. 1999, ApJ, 522, 1148
Priest, E. R., Heyvaerts, J. F., & Title, A. M. 2002, ApJ, 576, 533
Priest, E. R. & Schrijver, C. J. 1999, Sol. Phys., 190, 1
Schrijver, C. J., Hagenaar, H. J., & Title, A. M. 1997, ApJ, 475, 328
Schrijver, C. J., Title, A. M., Harvey, K. L., et al. 1998, Nature, 394, 152
Schwarzschild, M. 1948, ApJ, 107, 1
Spitzer, L. 1956, Physics of fully ionized gases (Interscience, New York)
Sturrock, P. A. & Uchida, Y. 1981, ApJ, 246, 331
Teriaca, L., Banerjee, D., & Doyle, J. G. 1999, A&A, 349, 636
van Ballegooijen, A. A. 1986, ApJ, 311, 1001
Wilhelm, K., Curdt, W., Marsch, E., et al. 1995, Sol. Phys., 162, 189
Wilhelm, K., Lemaire, P., Dammasch, I. E., et al. 1998, A&A, 334, 685
Withbroe, G. L. & Noyes, R. W. 1977, ARA&A, 15, 363
Wood, B. E., Linsky, J. L., & Ayres, T. R. 1997, ApJ, 478, 745
Young, P. R., Del Zanna, G., Landi, E., Dere, K. P., Mason, H. E., & Landini, M. 2003, ApJS, 144, 135